Selective Liposomal Transport Through Blood Brain Barrier Disruption in Ischaemic Stroke Reveals Two Distinct Therapeutic Opportunities

Authors: Zahraa S. Al-Ahmady *[1,2], Dhifaf Jasim[1], Sabahuddin Syed Ahmad[1], Raymond Wong[3], Michael Haley[3], Graham Coutts[3], Ingo Schiessl[3], Stuart M. Allan *[3] and Kostas Kostarelos *[1]

Affiliations:

[1] Nanomedicine Lab, Faculty of Biology, Medicine and Health, AV Hill Building, The Univerdsity of Manchester, Manchester M13 9PT, United Kingdom.

[2] Pharmacology Department, School of Science and Technology, Nottingham Trent University, Nottingham, NG11 8NS

[3]Lydia Becker Institute of Immunology and Inflammation, Division of Neuroscience and Experimental Psychology, School of Biological Sciences, Faculty of Biology, Medicine and Health, University of Manchester, Manchester Academic Health Science Centre, AV Hill Building, Manchester, M13 9PT.

*To whom correspondence should be addressed: zahraa.al-ahmady@ntu.ac.uk; stuart.allan@manchester.ac.uk; kostas.kostarelos@manchester.ac.uk

Supplementary Materials

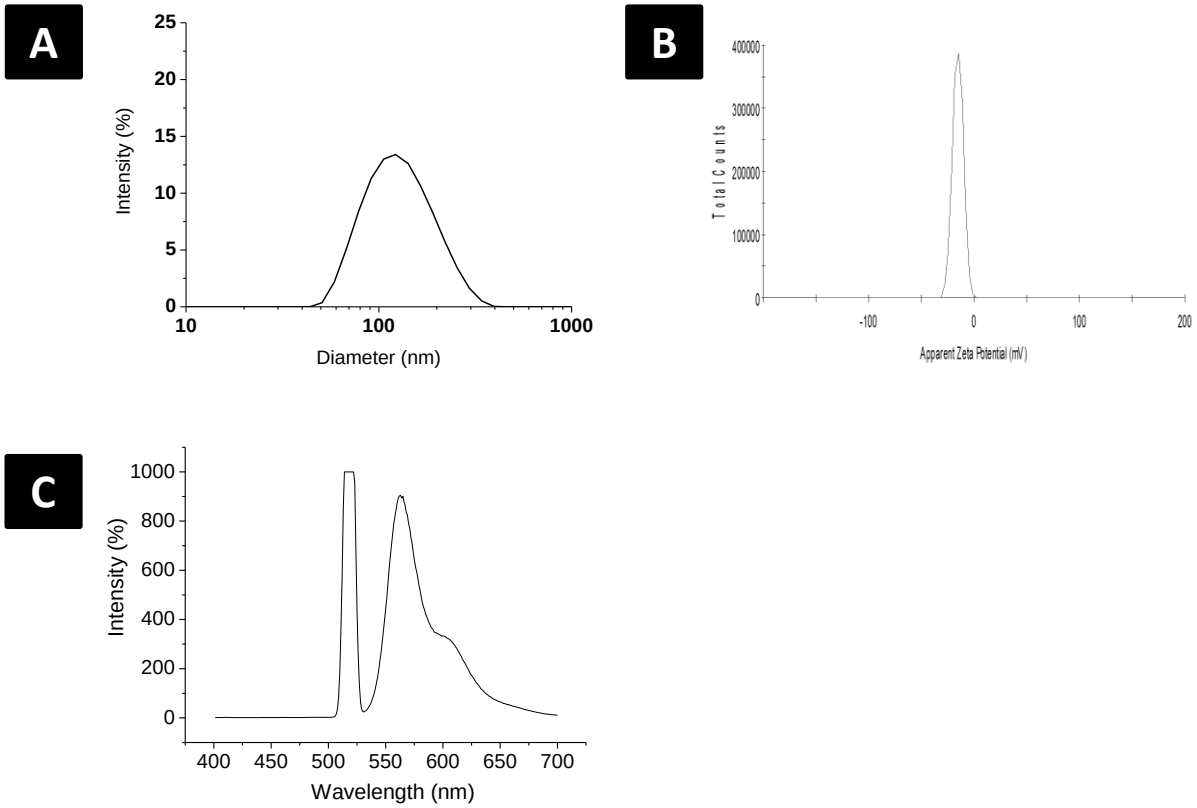

Figure S1: Physicochemical characterisation of DiI-Lp showing; (A) hydrodynamic diameter. (B) zeta potential and (C) fluorescent intensity at excitation wavelength of 518nm and emission wavelength 565 nm.

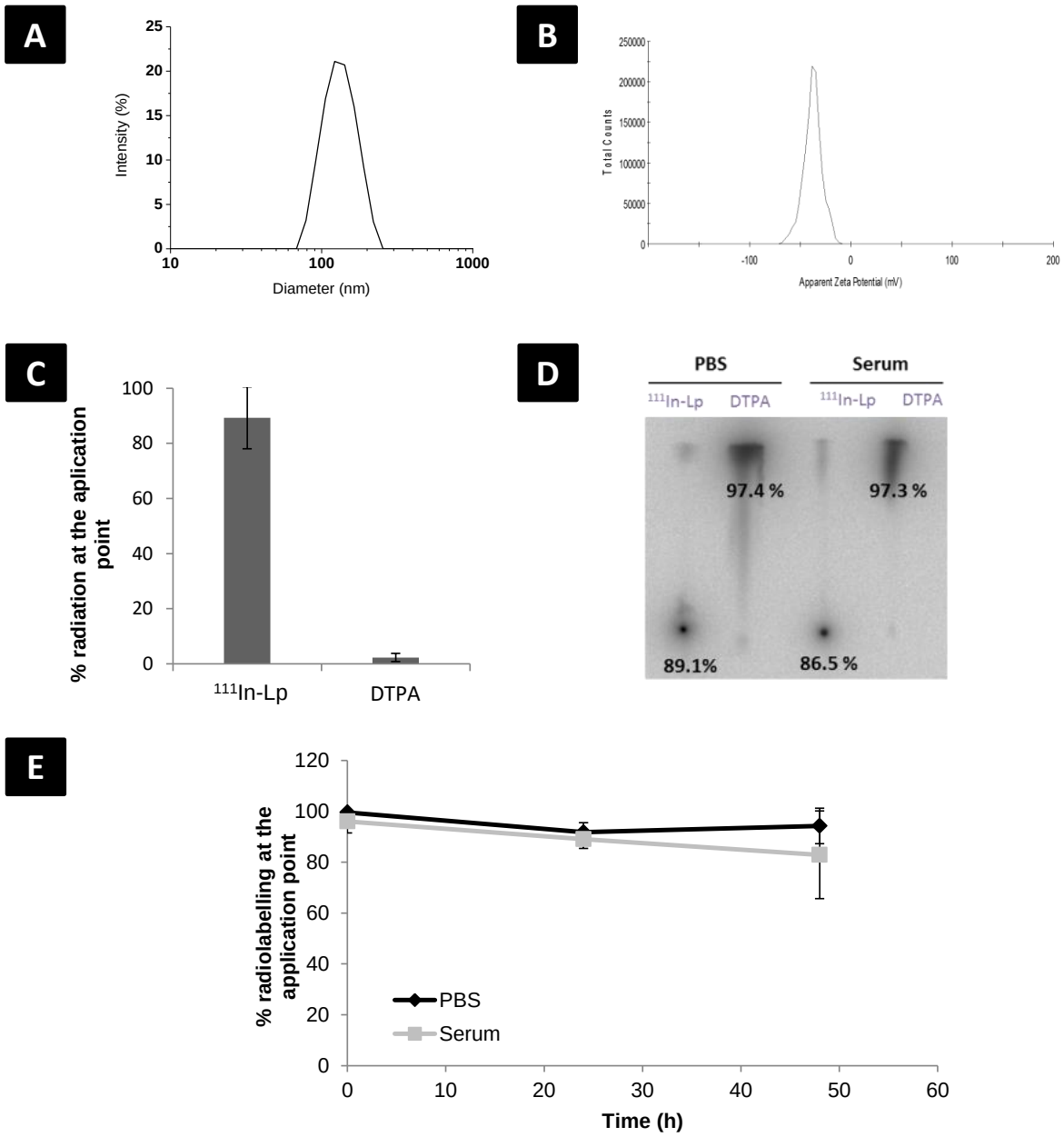

Figure S2: Characterisation of ^{111}In-Lp showing; (A) hydrodynamic diameter. (B) zeta potential, (C&D) radiolabelling efficiency and (E) radiolabelling stability overtime in PBS and 50% serum.

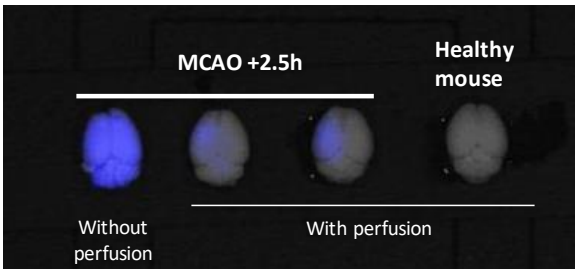

Figure S3: IVIS Lumina II imaging of the brain with and without transcardiac perfusion of the animals with PBS under terminal anaesthesia. Images show that in the absence of cardiac perfusion there is a nonspecific DiI-Lp signal throughout the brain. In contrast, animals with cardiac perfusion show selective accumulation of liposomes only in the ipsilateral hemisphere, in close proximity to the infarct.

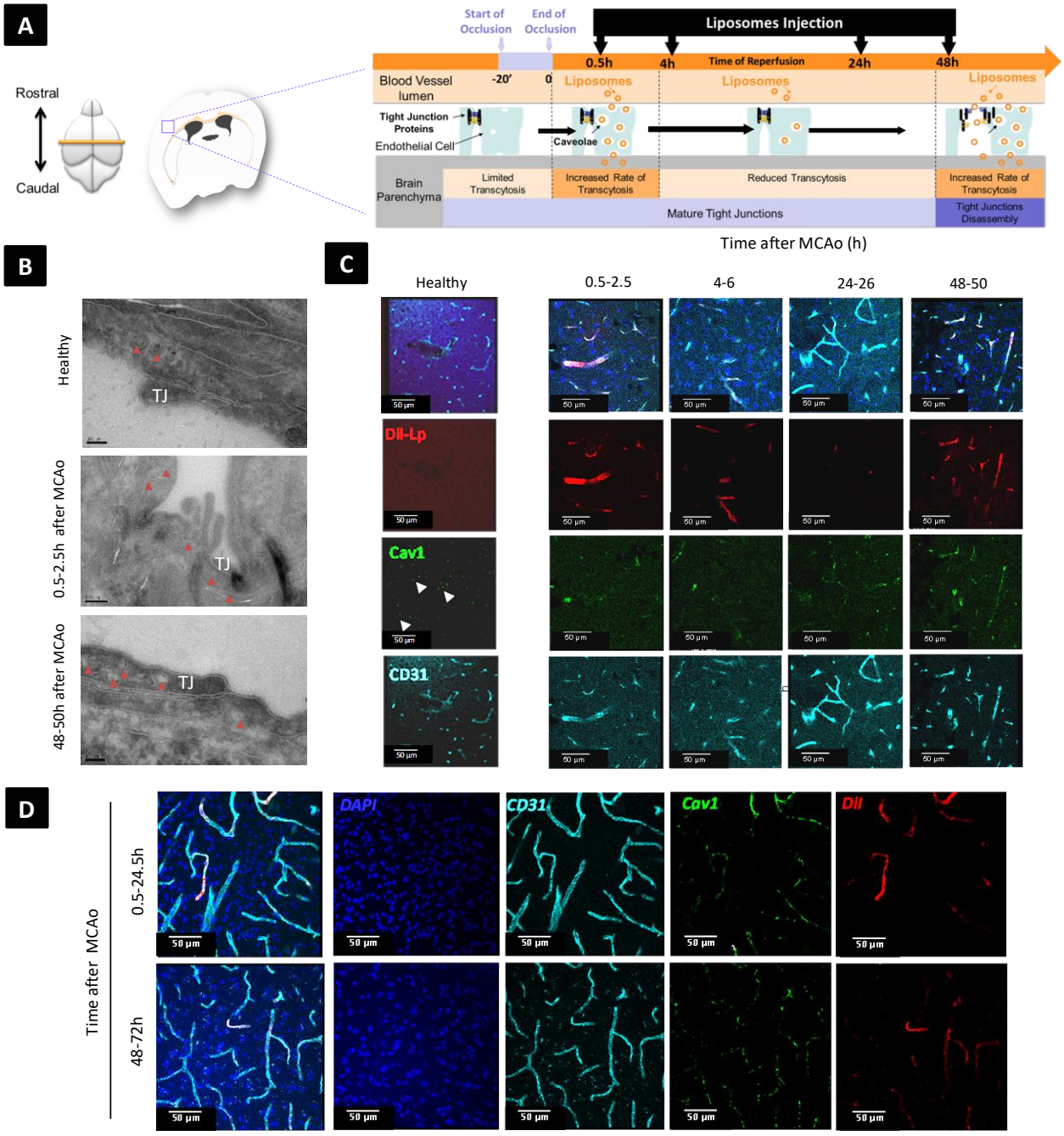

Figure S4: Selective liposomal accumulation into ischaemic cerebral cortex. (A) Schematic presentation of the experimental plan and the time frame for DiI-Lp intravenous administration after 20min of MCAo. (B) Ultrastructural changes in the brain endothelial cells in the cerebral cortex studied by EM early and late after MCAo and compared to naïve healthy brain. (C&D). White triangles indicate areas of low Cav1 expression in the healthy brain. Immunofluorescent staining showed co-localisation of DiI-Lp leakage with areas of enhanced Cav-1 expression when assessed both 2h and 24h after DiI-Lp I.V administration. Maximum DiI-Lp leakage detected when administered at 0.5h or 48h after MCAo indicating a biphasic window of therapeutic opportunities.

Cardiac perfusion was performed to remove any DiI-Lp that are still inside the blood vessels. Red arrows indicate the presence of transcytotic vesicles in the BECs.

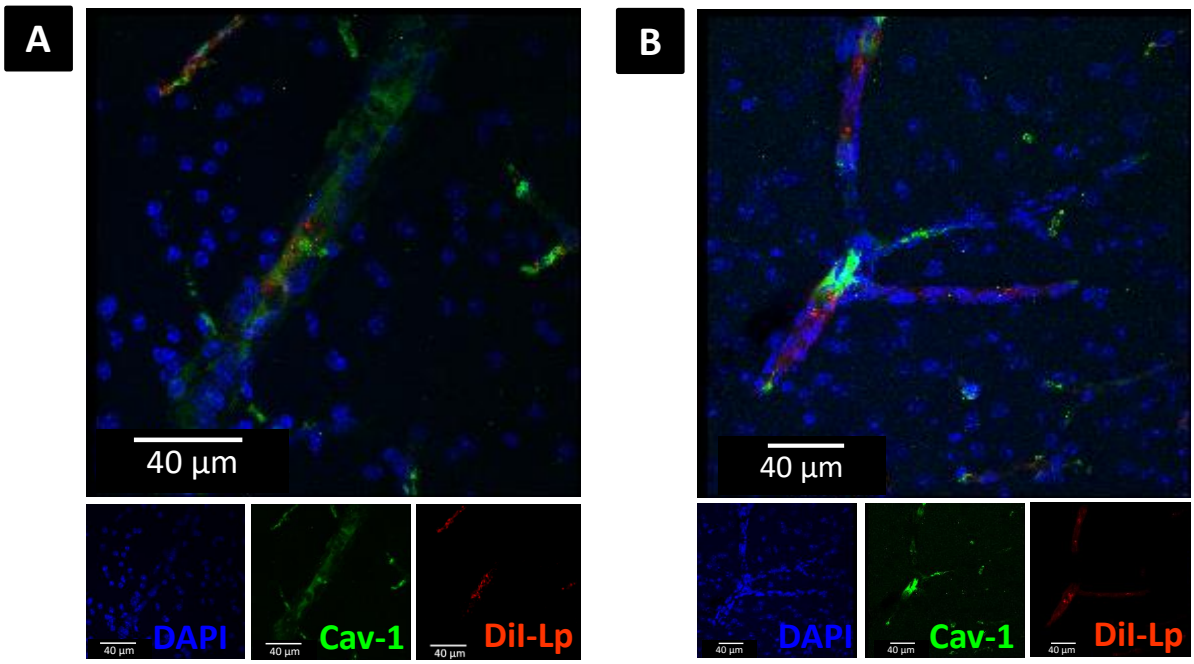

Figure S5: Selective liposomal accumulation into the ipsilateral striatum24h after DiI-Lp I.V administraion. Representative high magnification (100x with zoom factor 2) immunofluorescecet imaging of ipsilateral striatum at -0.58mm bregma showing DiI-Lp signal (red) inside Cav-1 positive vesicles of the brain endothelial cells. Confocal images were obtained 24h after I.V administration of DiI-Lp into MCAo mice at; (A) 0.5h and (B) 48h following reperfusion.

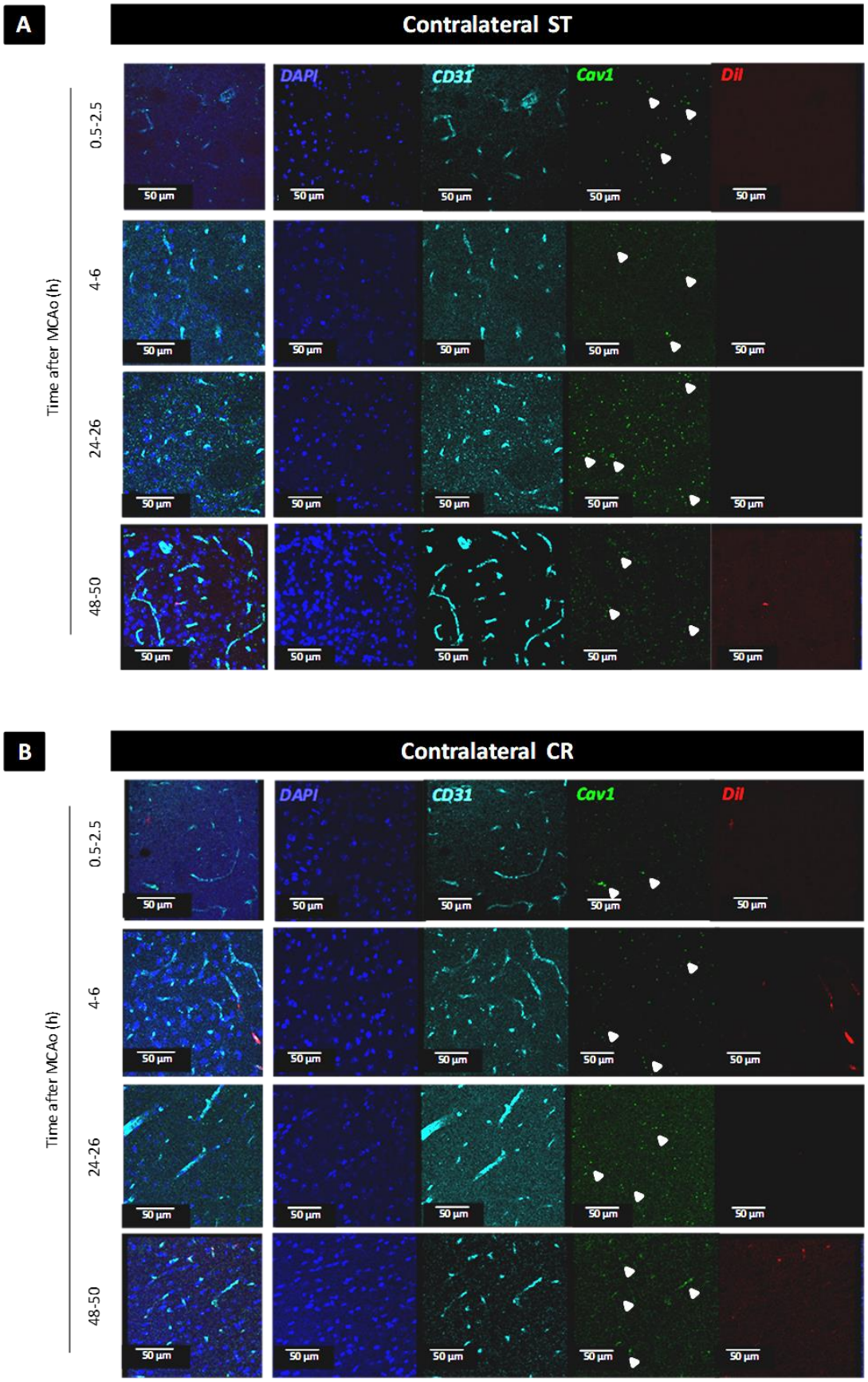
A
Contralateral ST
DAPI
CD31
Cav1
DiI
Time after MCAo (h)
0.5-2.5
4-6
24-26
48-50
50 μm
B
Contralateral CR
DAPI
CD31
Cav1
DiI
Time after MCAo (h)
0.5-2.5
4-6
24-26
48-50
50 μm

Figure S6: Confocal images of (A) contralateral striatum (ST) and (B) contralateral cortex (CR) indicated minimum expression of Cav-1 and no DiI-Lp accumulation which confirm the selective accumulation of liposomes into the brain after ischaemic stroke. Images were obtained 2h following DiI-Lp I.V administration. White triangles indicate areas of low level Cav1 expression.

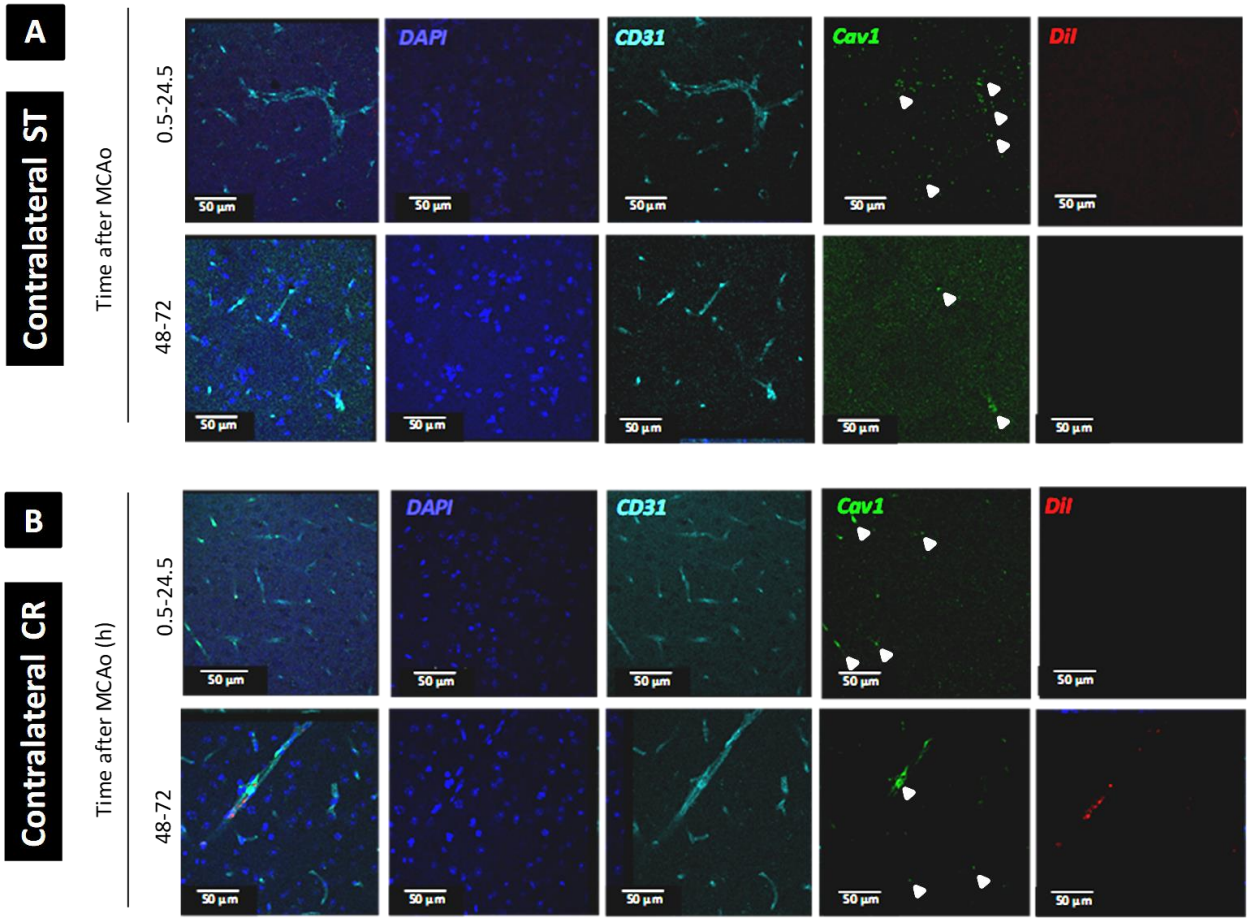

Figure S7: Confocal images of (A) contralateral striatum (ST) and (B) contralateral cortex (CR) 24h after DiI-Lp I.V administration into MCAo mice at 0.5h or 48h after reperfusion Images indicated limited Cav-1 expression and no DiI-Lp accumulation. White triangles indicate areas of low level Cav1 expression.

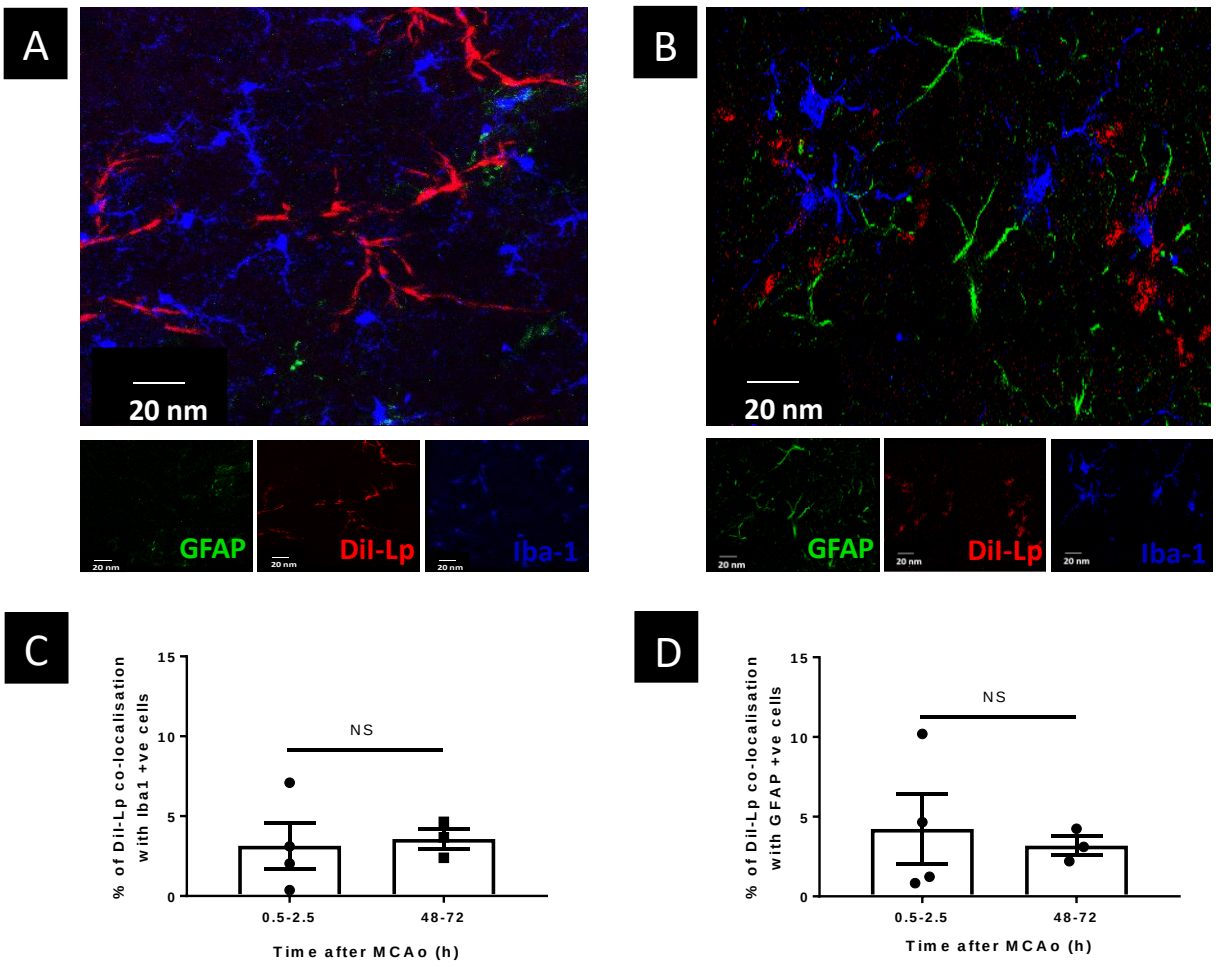

Figure S8: Evaluation of DiI-Lp co-localisation with microglia and astrocytes in the ipsilateral cortex. Representative confocal images showing co-localisation of DiI-Lp with of Iba1 (activated microglial marker) and GFAP (astrocytes marker). Brain sections were analysed 24h following the injection of DiI-Lp intravenously into MCAo mice in the; (A) early phase (MCAo+0.5h) and (B) delayed phase (MCAo+48h) after reperfusion. Quantification of DiI-Lp co-localisations with (C) Iba-1 and (D) GFAP indicated <5% co-localisation with both markers.

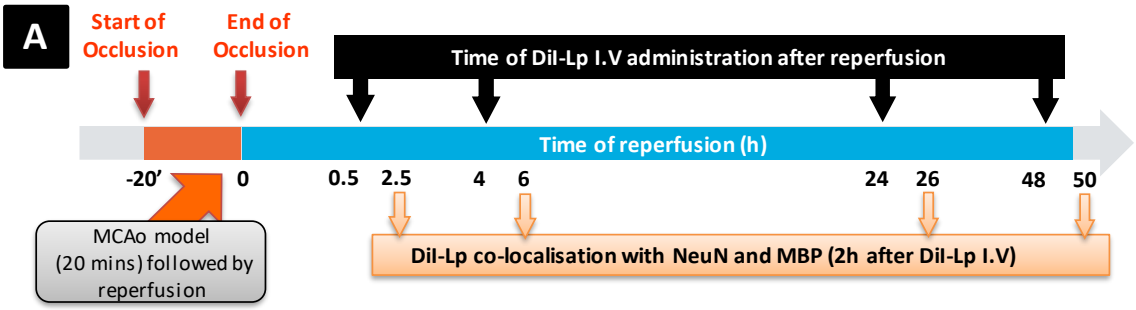
A
Start of Occlusion
End of Occlusion
Time of DiI-Lp I.V administration after reperfusion
Time of reperfusion (h)
-20'
0
0.5
2.5
4
6
24
26
48
50
MCAo model (20 mins) followed by reperfusion
DiI-Lp co-localisation with NeuN and MBP (2h after DiI-Lp I.V)

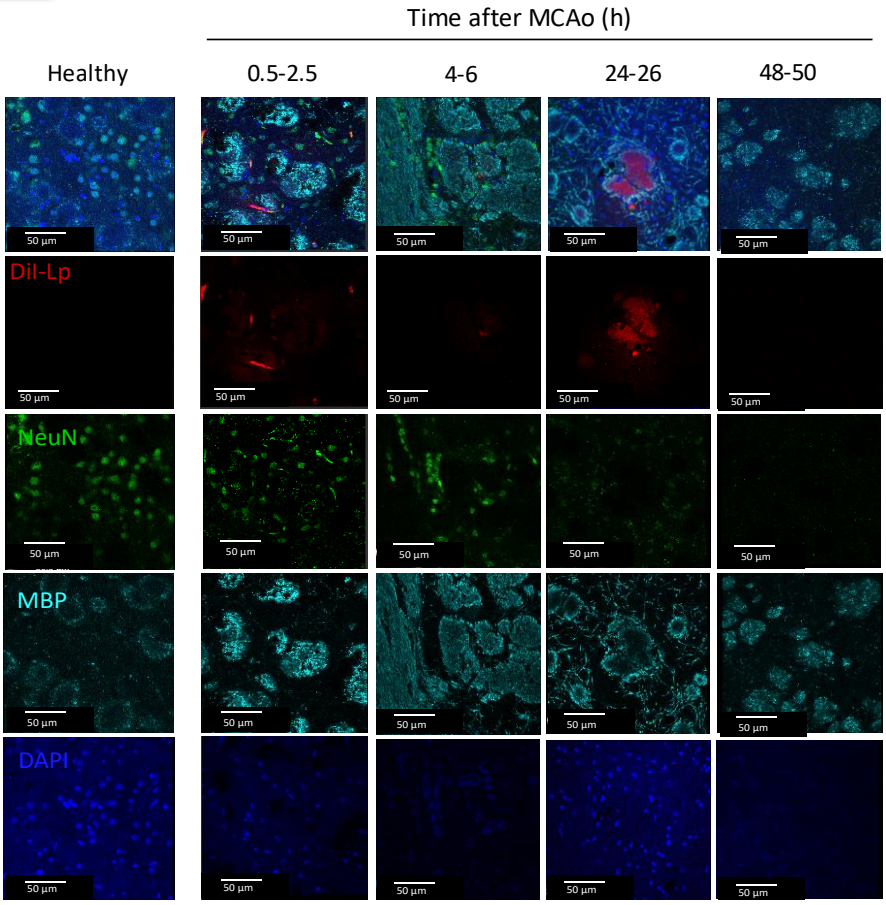
Time after MCAo (h)
Healthy
0.5-2.5
4-6
24-26
48-50
DiI-Lp
NeuN
MBP
DAPI
50 µm

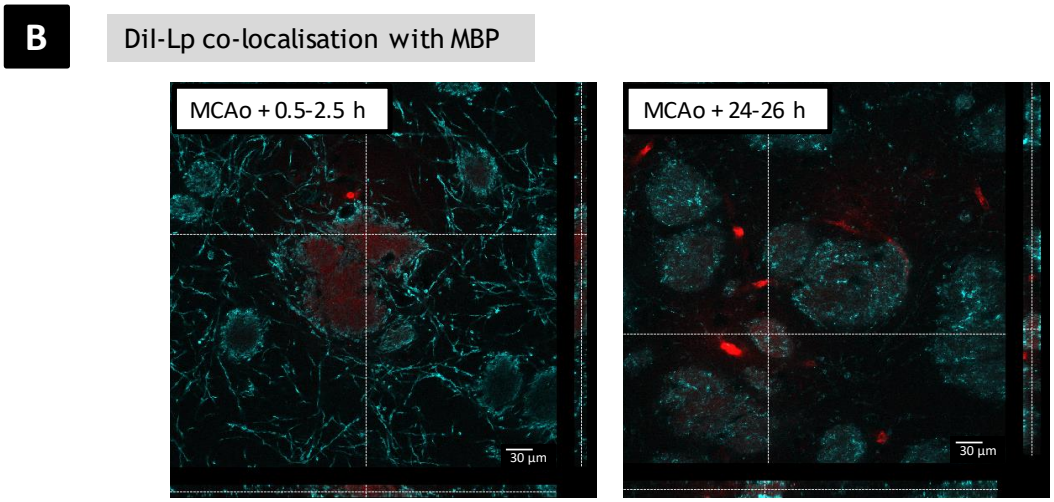
B
DiI-Lp co-localisation with MBP
MCAo + 0.5-2.5 h
MCAo + 24-26 h
30 µm

Figure S9: Confocal images of DiI-Lp co-localisation with Neurons and oligodendrocytes in the ipsilateral striatum. A) 2h following DiI-Lp I.V administration into MCAo mice indicating no clear co-localisation of DiI-Lp with Neurons (green) and occasional co-localisation with oligodendrocytes (Cyan). B) Representative images of DiI-Lp co-localisation with MBP marker.

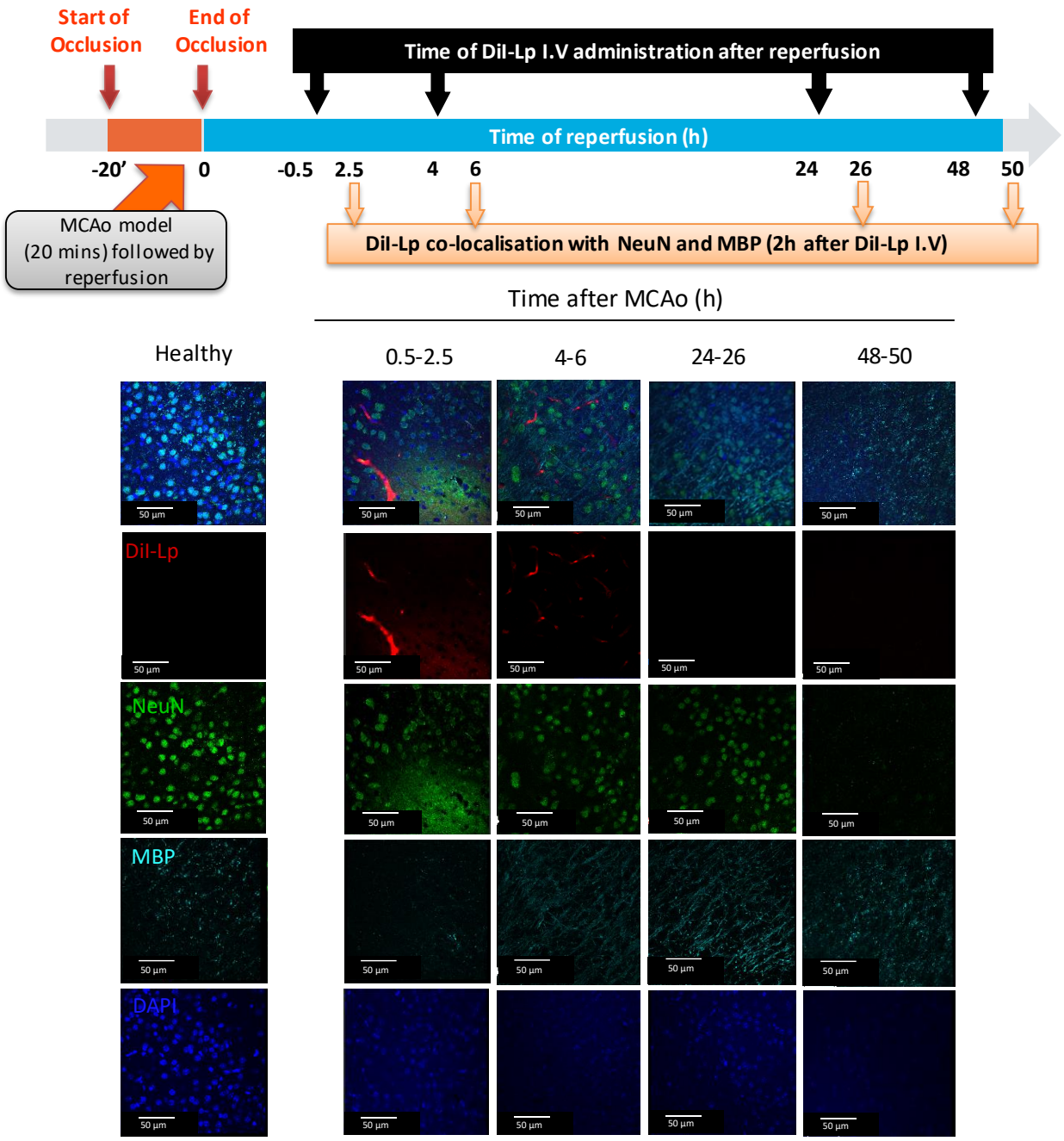

Figure S10: Confocal images of DiI-Lp co-localisation with Neurons and oligodendrocytes in the ipsilateral cortex 2h following DiI-Lp I.V administration into MCAo mice indicating no clear co-localisation of DiI-Lp with Neurons (green) and oligodendrocytes (Cyan).